KUFA JOURNAL OF ENGINEERING
ISSN 2071-5528
PRINTED IN IRAQ

Volume 4, Number 2 pp.29-51, 2013

Non-Linear Finite Element Analysis of Prestressed Concrete Members Under Torsion

Dr. Ihsan A.S. Al-Shaarbaf *University of Baghdad*

Dr. Ali N. Attiyah *University of Kufa*

Mustafa S. Shuber *University of Kufa*

(Received:17/4/2012 ; Accepted :21/2/2013)

Abstract:

This paper is devoted to investigate the behavior of prestressed concrete beams under pure torsion using a non-linear three-dimensional finite element model. The 20-noded isoparametric brick elements have been used to model the concrete. The reinforcing bars are idealized as axial members embedded within the concrete element and perfect bond between the concrete and the reinforcement has been assumed to occur.

The behavior of concrete in compression is simulated by an elasto-plastic work hardening model followed by a perfect plastic response, which is terminated at the onset of crushing. On the other hand the behavior in tension is simulated by implementing a smeared crack model in connection with using a tension-stiffening model that account for the retained post-cracking stresses, and a shear retention model that modifies the shear modulus of rigidity as the crack widens. Also a model to simulate the reduction in the concrete compressive strength in presence of tensile transverse straining has been implemented in this study. Two types of prestressed concrete beams under torsion have been analyzed and the finite element solutions were compared with the experimental data. Several parametric studies have been carried out to investigate the effect some important material parameters. In general, good agreement between the finite element solutions and the experimental results was obtained.

التحليل غير الخطي باستخدام طريقة العناصر المحددة للأعضاء الخرسانية تحت تأثير عزم اللي

تم في هذا البحث استقصاء سلوك العتبات الخرسانية المسبقة الجهد المعرضة لعزوم اللي باستعمال طريقة العناصر المحددة واستخدام نموذج ثلاثي الابعاد لإجراء التحليل غير الخطي. اختير العنصر الثلاثي الابعاد ذي العشرين عقدة لتمثيل الخرسانة اما حديد التسليح فقد تم تمثيلة عاى شكل عناصر احادية البعد مطمورة داخل العنصر ذو العشرين عقدة واعتمدت فرضية الترابط الكلي بين مادتي الخرسانة وحديد التسليح خلال جميع مراحل تسليط الاحمال. تم اعتبار الخرسانة على انها مادة تتصرف تصرفا " مرنا " تحت تأثير اجهادات الضغط في بداية التحميل يتبعه تصرفا " مرنا-لدنا " وعندما تصل الاجهادات في الخرسانة الى الاجهاد الاقصى تسلك سلوكا " تام اللدونة " ولغاية الفشل. اما سلوك الخرسانة تحت تأثير اجهادات الشد فقد تم تبني انموذج التشقق المنتشر.، مع الاخذ بالحسبان الاجهادات المتبقية في مرحلة ما بعد التشقق وتم استخدام انموذج تصلب الشد Tension Stiffening Model لهذا الغرض وكذلك استخدم انموذج احتباس القص Shear Retention Model لتخفيض قيمة معامل صلابة القص Shear Rigidity Modulus مع استمرار زيادة عرض الشق واستعمل ايضا انموذجا يأخذ بنظر الاعتبار التقليل من مقاومة الخرسانة للانضغاط بسبب وجود انفعالات الشد في قضبان حديد التسليح المستعرضة. تم تحليل ثلاثة انواع من الاعضاء الخرسانية مسبقة الجهد تحت تأثير عزوم اللي وتم مقارنة النتائج المستحصلة من طريقة العناصر المحددة مع النتائج المختبرية. أجريت تجارب عديدة لدراسة تأثير بعض المتغيرات المهمة كتلك المتعلقة بنمذجة وتمثيل خواص الخرسانة المسبقة الجهد، وتلك المرتبطة بطريقة التحليل للعناصر المحددة. على سلوك وسعة العتبات الخرسانية المسبقة الجهد تحت تأثير اللي. فقد درس تأثير العديد من المتغيرات لبيان تأثيرها في تصرف العتبات. بصورة عامة كان التطابق جيدا بين النتائج العملية وطريقة العناصر المحددة.

1- Introduction:

Torsion is a major factor to consider in the design of many kinds of reinforced concrete structures, including space frames, beams that support cantilever slabs or balconies, horizontally curved beams, spiral staircases, skew bridges … etc. However despite the fact that torsional stresses can frequently occur, torsion was generally ignored in design of reinforced concrete members before the 1960s. The large safety factors incorporated in flexure design were assumed to be sufficient to accommodate the effect of torsion. This assumption has been responsible for many cases of torsional distress and failure(1).

Prestressing can be defined in general terms as the pre loading of a structure before the application of the service load, so as to improve its performance in specific ways(2). Although several patents were taken out in the last century for various prestressing schemes, they were unsuccessful because low-strength steel was used. It was only in the early part of the twentieth century that the French engineer Eugene Freyssinet approached the problem in a systematic way and using high-strength steel, first applied the technique of prestressing concrete successfully. Since then prestressed concrete has become a well established method of construction and the technology is available in most developed and in many developing countries(3). Currently, no design criteria to obtain the torsional capacity of prestressed concrete beam under torsion are available in current ACI code 318-99.

At present, with the development of digital computers and numerical techniques, the finite element method has emerged as a powerful analytical tool for analysis of structures. This has opened a spacious world for engineers to model rationally many aspects of the phenomenological behaviors encountered in prestressed concrete. These aspects include the nonlinear multiaxial material properties, modeling of cracking and crushing, the changes in material properties after cracking and crushing, yielding of prestressed steel and many other properties.

2- Finite Element Model:

2-1 Material Representation:

2-1-1Concrete idealization: The three dimensional modeling is adopted in the present study. The twenty-noded hexahedral isoparametric elements have been used. The element has its own local coordinate system, r, s ,t shown in Fig. (1), with the origin at the center of the element such that each local coordinate ranges from (-1) to (+1).

2-1-2 Reinforcement representation: This study adopts the embedded representation of prestressing shown in Fig.(1) which is almost used in connection with the higher order isoprametric concrete elements. The prestressing bar is considered to be an axial member built into the isoparmetric concrete element such that its displacements are consistent with those of the element. Perfect bond has been assumed between concrete and prestressing steel bars.

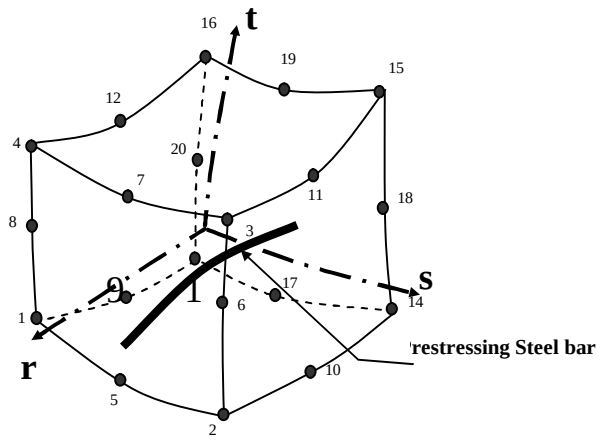

Fig.(1) The 20-noded brick element and embedded reinforcement in local coordinate system.

2-2 Numerical Integration :

The evaluation of the stiffness matrices and the equivalent nodal loads involves multiple integration. Explicit integration for these functions may be very difficult or even impossible. Therefore, an alternative arrangement of numerical integration is usually used. The 15 Gauss quadratic integration rule has been used in this investigation. The relative positions of the sampling points for this rule over the volume of the brick element are shown in Fig.(2).

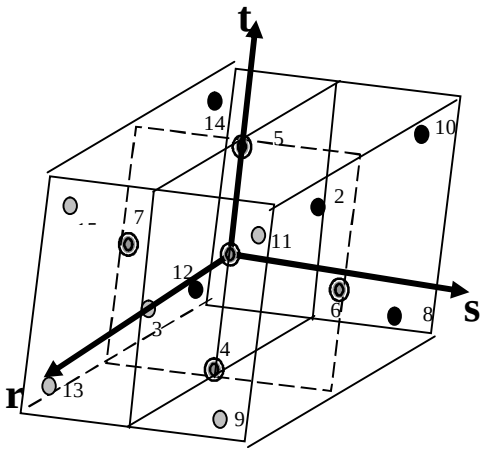

Fig.(2) Distribution of the sampling points over the element using the 15-points

2-3 Nonlinear Solution Techniques:

The Incremental-Iterative method is the most commonly used technique for solving non-linear finite element problems. It implies the subdivision of the total external load into smaller increments, within each increment of loading iterative cycles are performed in order to obtain a converged solution corresponding to the stage of loading under consideration Fig.(3).

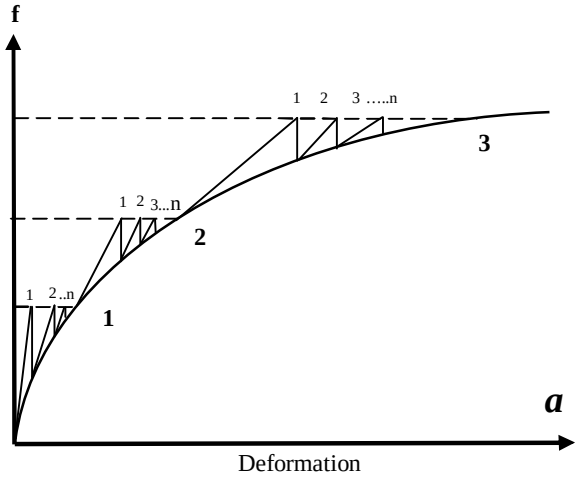

Fig.(3) Incremental- Iterative Techniques

2-4 Convergence Criterian:

The force convergence criterion has been considered in the numerical analyses carried out in the present work. When the residual (out of balance) forces are stifficiently small, the convergence is assumed to occur. Hence this criterion can be expressed in the from:

$$\frac{\sqrt{\{r(a)\}^T \cdot \{r(a)\}}}{\sqrt{\{f\}^T \cdot \{f\}}} \leq \textit{Converg.Tol}\textbf{erance} \quad \text{.....(1)}$$

2-5 Equivalent Nodal Forces:

An iterative scheme can be in used to determine the proper distribution of nodal loads corresponding to elastic pure torque. The procedure is based on the fact that the restrained end represents a section remote from the loaded end, therefore the reaction forces at the nodes of the restrained end are a better estimate of the correct loads than the corresponding nodal loads at the free end. When the applied loads are correct than the corresponding reaction forces at the

restrained end will have the same magnitude and opposite direction. The iterative scheme is illustrated by the following steps:

a) A set of nodal loads is applied at the loaded end such that the resulting torque equals the required applied torque. In general the distribution of the nodal loads will not be the correct one.

b) The reactions corresponding to the above loading at the restrained end are determined using the finite element analysis.

c) The reactions are then used as a new set of nodal loads at the loaded end.

d) Steps b and c are then repeated until the difference between each nodal forces at the loaded end and the corresponding reactions at the restrained end is negligibly small.

The scheme has been carried out for each beam analyzed in this study prior to the nonlinear analysis. The resulting sets of nodal loads are then used in the nonlinear analysis to represent as the external torque.

3-Modeling of Material Properties:

3-1 Behavior of Concrete in Compression:

The accuracy of the numerical material models that may be adopted in the analysis should trace the overall behavior of the member within sufficient degree of accuracy. In the presented study, the stress-strain curves in compression is simulated by an elastic-plastic work hardening response followed by a perfectly plastic response, which is terminated at the onset of crushing. The plasticity model is expressed in terms of, the yield criterion, hardening rule, flow rule and crushing condition.

3-1-1 The yield criterion: In order to mark the onset of plastic deformation of a material under multiaxial state of stress, a yield criterion is required. The yield criterion for concrete under a triaxial state of stress is generally assumed to be dependent on three stress invariants, However, many studies[3] showed that a yield criterion can be adequately expressed in terms of two-stress invarients only as

$$f(\sigma) = CI_1 + \sqrt{(CI_1)^2 + 3\beta J_2} = \sigma_o \quad \text{.....(2)}$$

where C , β are material parameters and I_1 , J_2 are the first stress invariant and the second deviatoric stress invariant, respectively that are given by:

$$I_1 = \sigma_x + \sigma_y + \sigma_z \quad \text{.....(3)}$$

$J_2 = \frac{1}{3}\left[\left(\sigma_x^2 + \sigma_y^2 + \sigma_z^2\right) - \left(\sigma_x.\sigma_y + \sigma_y\,\sigma_z + \sigma_z\,\sigma_x\right)\right] + \tau_{xy}^2 + \tau_{yz}^2 + \tau_{zx}^2$ and σ_o is the equivalent effective stress at the onset of plastic deformation which can be determined from uniaxial compression test as

$$\sigma_o = C_p \; f_c' \qquad \text{.....(4)}$$

where C_p is a plasticity coefficient which is used to mark the initial of plastic deformation**.**

3-1-2 The hardening rule: The hardening rule is necessary to define the change of positions of the loading surfaces during the plastic deformation. A relationship between the accumulated plastic strain and the effective stress is required to control the position of the current loading surface. A number of hardening rules have been proposed to describe the growth of the subsequent loading surfaces for a work hardening material.(3)

In the current study an isotropic hardening rule is adopted. Therefore, from equation (2), the subsequent loading surfaces may be expressed as:

$$f(\sigma) = C.I_1 + \sqrt{(C.I_1)^2 + 3\beta J_2} = \sigma' \qquad \text{.....(4)}$$

where σ' represents the stress level at which further plastic deformation will occur. The effective stress-plastic strain relationship can be expressed as:

$$\sigma' = C_p \,.\, f_c' - E.\varepsilon_p + \sqrt{2E^2.\varepsilon_o'\varepsilon_p} \qquad \text{.....(5)}$$

where ε_o' is total strain shown in Fig.(4).

The uniaxial stress-strain curve is assumed to be linear up to a stress level equals to $C_p \; f_c'$ followed by a parabolic shape up to the peak compressive stress f_c'. In the present study, values of ***0.3*** and 0.5 are assumed for plastic coefficient C_p for normal and high strength concrete respectively. The plastic yielding begins at a stress level of $C_p \; f_c'$. If C_p = ***1.0*** , then the elastic perfectly plastic behavior is specified, as shown in Fig.(4).

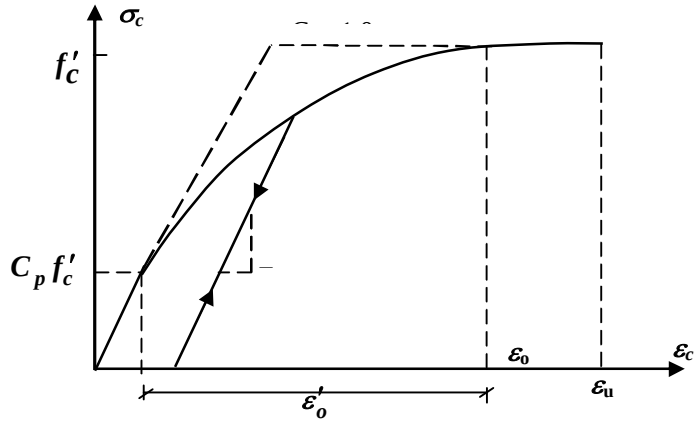

Fig.(4) Uniaxial stress-strain curve of concrete in compression

3-1-3 The flow rule: In order to connect the loading function f and the stress-strain relation in the plastic range, an associated flow rule is usually employed. This means that the plastic deformation rate vector will be assumed to be normal to yield surface. The plastic strain increment is defined as[4].

$$d\{\varepsilon_p\} = d\lambda \frac{\partial f(\{\sigma\})}{\partial \{\sigma\}} \qquad \text{.....(6)}$$

The normal to the current loading surface $\partial f(\{\sigma\})/\partial\{\sigma\}$ is termed the flow vector. The yield function derivatives with respect to the stress components define the flow vector $\{a\}$ as:

$$\{a\} = \left\{ \frac{\partial f}{\partial \sigma_x}, \frac{\partial f}{\partial \sigma_y}, \frac{\partial f}{\partial \sigma_z}, \frac{\partial f}{\partial \tau_{xy}}, \frac{\partial f}{\partial \tau_{yz}}, \frac{\partial f}{\partial \tau_{zx}} \right\}^T$$

3-1-4 Crushing condition: in the adopted model, the isotropic expansion of the subsequent loading surfaces is terminated when the effective stress reaches the peak compressive stress. Beyond that a perfectly plastic response is assumed to occur. The perfectly plastic flow continues until the ultimate deformation capacity of concrete is reached and the material eventually exhibits a crushing failure. The stresses at crushed sampling point drop abruptly to zero. The crushing criterion is obtained by simply converting the yield criterion in equation (2), which is written in terms of stresses directly into strains, thus:

$$C.I'_1 + \sqrt{(C.I'_1)^2 + 3.\beta\ J'_2} = \varepsilon_{cu} \qquad \text{.....(7)}$$

where I_1' and J_2' are first the strain and second deviator strain invariants, ε_{cu} is the ultimate crushing strain of concrete, extrapolated from uniaxial test.

3-2 Behavior of concrete in tension

3-2-1 The cracking criterion : In the present study, the initiation of cracking is controlled a maximum tensile stress criterion. At the sampling point under consideration, if the major principal stress, σ, exceeds the limiting tensile strength a crack is assumed to form. The limiting tensile stress required to define the onset of cracking can be calculated for state of triaxial tensile stress and for combinations of tension and compression principal stresses as follows.

a) For the triaxial tension zone :

$$\sigma i = \sigma_{cr} = f_t \qquad \text{i = 1, 2, 3}$$

b) For the case of the tension-tension-compression zone:

$$\sigma_i = \sigma_{cr} = f_t \left[1.0 + \frac{0.75\sigma_3}{f_c'} \right] \qquad \text{i = 1, 2}$$

c) For the case of tension-compression- compression zone.

$$\sigma_i = \sigma_{cri} = f_t \left[1.0 + \frac{0.75\sigma_2}{f_c'} \right] . \left[1.0 + \frac{0.75\sigma_3}{f_c'} \right]$$ where, σ_{cr} is the cracking stress and f_t , f_c' are the tensile and compressive concrete strength (positive values).

3-2-2 Tension stiffening model: The tension stiffening effect is found to be quite significant under service load conditions by increasing the overall stiffness of the system in the post cracking range. In finite element modeling of reinforced concrete two approaches have been suggested to account for this effects[5]. The first approach is characterized by increasing the stiffness of steel bars. The second approach is characterized by a gradual decrease of the tensile stress in the cracked concrete over a specified strain range. Many researchers[6,7] used the second approach to account for the tension-stiffening effect conventionally reinforced concrete members.

In a current work, the second approach is adopted to represent the tension-stiffening effect. The adopted tension stiffening the model is shown in Fig.(5).

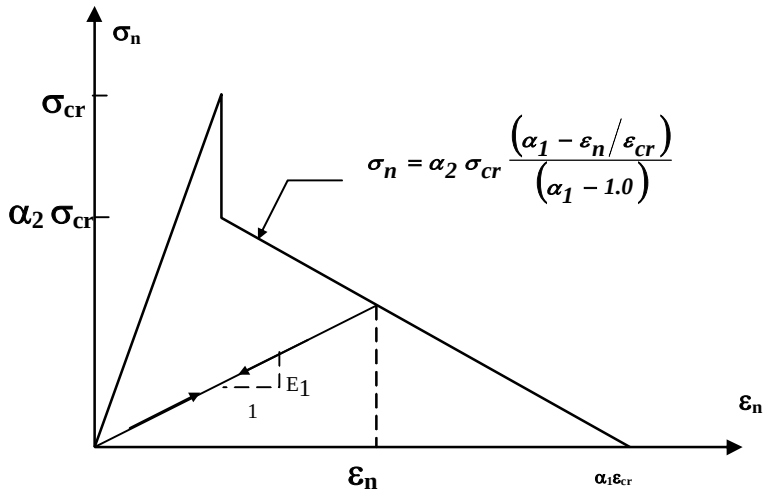

Fig.(5): Post-cracking model for concrete in tension[6].

3-3 Modelling of steel reinforcement

Prestressing steel bars can be assumed to transmit axial forces only. Modeling of ordinary and prestressing steel in connection with the finite element analysis of prestressed concrete members is much simpler than the modeling of concrete.

In the present research work, the uniaxial stress-behavior of ordinary and prestressing steel bars has been simulated by an elastic linear work hardening model, Fig.(6).

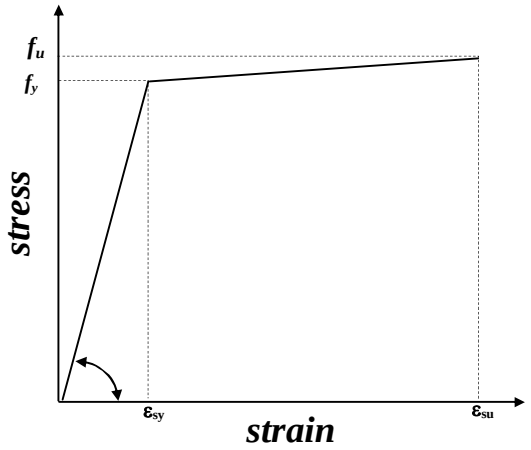

Fig.(6): Stress-strain curve for prestressing steel bars used in the analysis

4- Numerical Examples

To demonstrate the applicability of the method developed in the present study to the analysis of prestressed concrete members two examples are presented. .

4-1 Hsu Prestressed Concrete beam

Hsu[29] tested a series of rectangular prestressed concrete beams with various properties and details of reinforcement. Among these tested specimens, the beam designated as (P8) was selected for present research work in order to test the ability of the finite element model in predicting behavior of prestressed concrete members subjected to torsional loading.

4-1-1 Geometry and materiel properties: The chosen simply supported beam had a rectangular cross- section, the cross section was 254mm wide 381mm deep. The beam was 2000mm long. An increasing lateral load was applied at the ends of the beam. Details of the beam are given in Fig.(6). The material properties and the additional material parameters adopted in the analysis are given in Table (1).

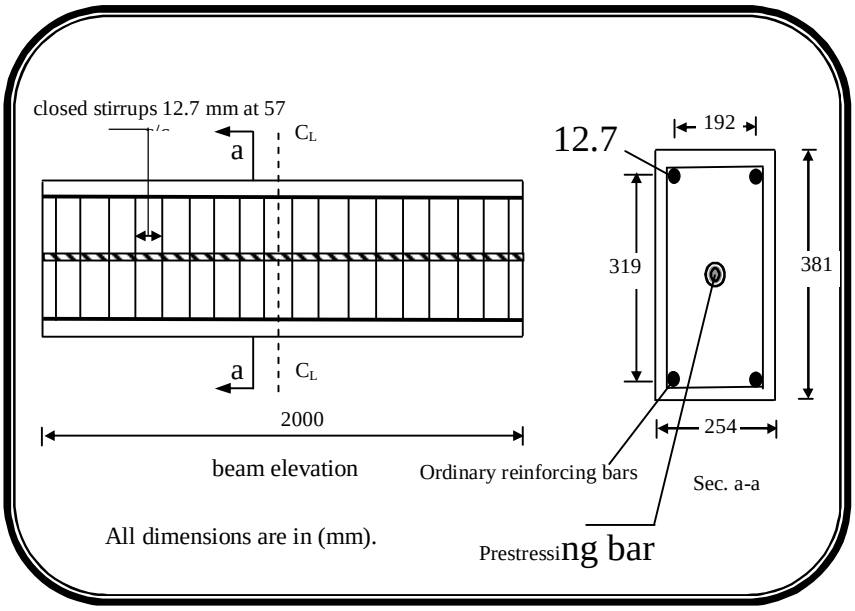

Fig.(6): Hsu beam (P8), dimensions and reinforcement details.

Table (1): Material properties for Jack et al. prestressed concrete beam.

Concrete
Young's modulus (N/mm^2) …… E_c = 26000
Poisson's ratio …… …ν = 0.2
Compressive strength (N/mm^2) … .. f'_c = 31.0
Tensile strength (N/mm^2) … … ……f_t = 3.2
Tension stiffening parameters …. α_1 =10 α_2 = 0.6
Prestressing steel
Young's modulus (N/mm^2) …… E_s =200000
Yield stress (N/mm^2) … …… f_{py} =897
Ultimate stress (N/mm^2) …… f_{pu} =1103.2
Longitudinal Reinforcement
Young's modulus (N/mm^2) …….. E_c = 200000
Yield stress (N/mm^2) …….. F_y = 334.4
Area of longitudinal reinforcement (mm^2)… 129
Transverse Reinforcement
Young's modulus (N/mm^2) …….. E_c = 200000
Yield stress (N/mm^2) …….. F_y = 336
Area of longitudinal reinforcement (mm^2)… 129

4-1-2 Finite element idealization: Because the beam was tested under pure torsion, a segment representing half the length of the beam has been considered in the analysis. This segment was modeled using a finite element mesh of eight quadratic brick elements.

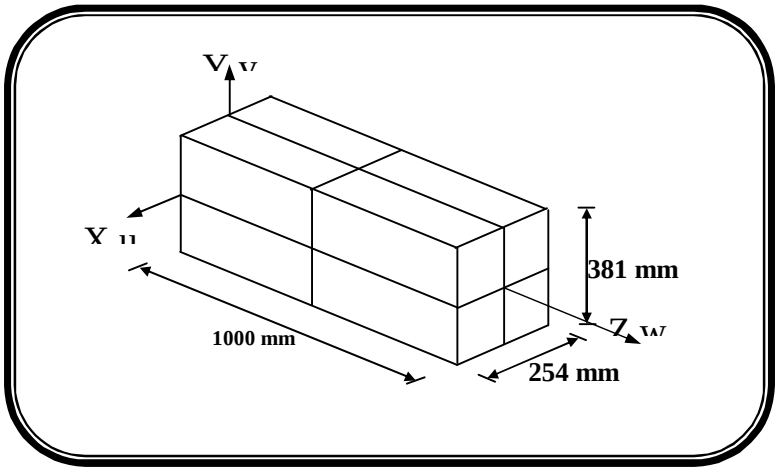

Fig.(7): Hsu beam, finite element mesh (8 elements).

4-1-3 Results of the analysis: The experimental and numerical torque-twist curves obtained for this beam are shown in Fig.(8). The figure indicates good agreement between the finite solution and the experimental results throughout the entire range of loading. The ultimate torque obtained from the numerical analysis was (63.09 kN.m) while that obtained from the experimental results was (61.7 kN.m). The ratio of the predicted ultimate torque to the corresponding experimental torque is (1.02).

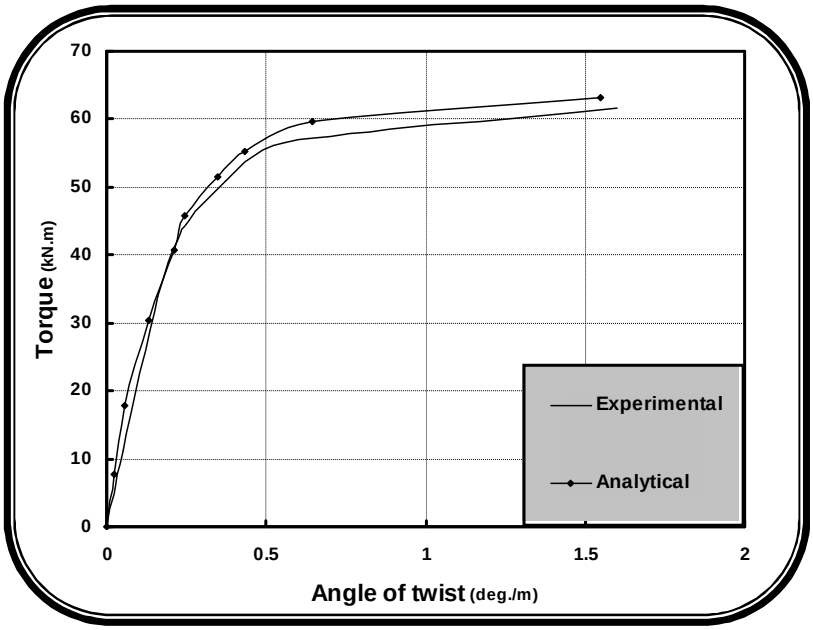

Fig.(8): Hsu beam (P8), experimental and analytical torque-twist curves.

4-2 wafa et al. prestressed rectangular beam (B0.0-2a): Wafa et al. tested a series of 18 rectangular concentrically prestressed concrete beams with and without fiber reinforcement subjected to torsion. One of these beams has been selected for the present study. This beam is designed as (B0.0-2a) and was cast without fiber reinforcement.

4-2-1 Geometry and materiel properties: The total length of test specimen of 2190 mm with 100 * 250 mm rectangular cross section. The effective span of tested beam was 1850 mm. The beam was concentrically prestressed with 12.7 mm prestressed strand without any additional ordinary longitudinal bars or stirrups, Dimensions and reinforcement details of the beam are given in Fig.(9).

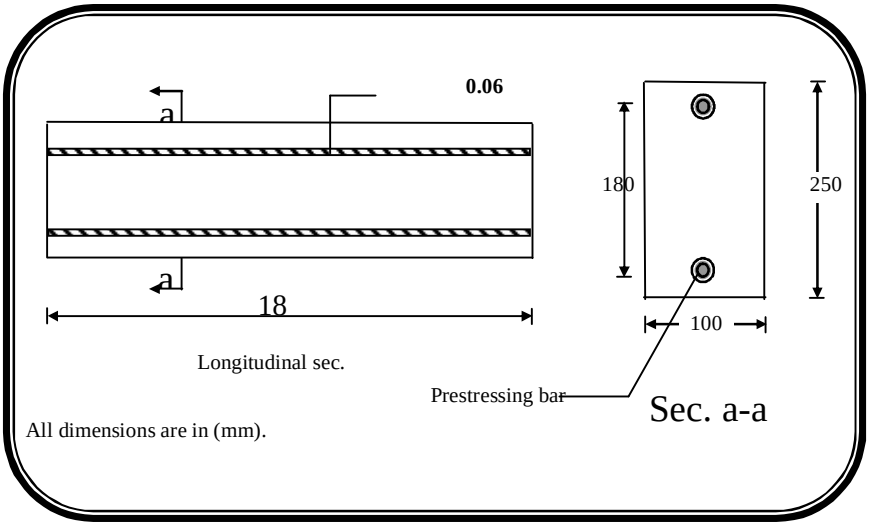

Fig.(9): Wafa et al. beam (B0.0-2a), dimensions and reinforcement details

The material properties and the addition parameters adopted in the analyses are given in Table (2)

Table (2): Material properties for Jack et al. prestressed concrete beam.

Concrete	
Young's modulus (N/mm^2) ……	E_c =28400
Poisson's ratio …… …	ν = 0.2
Compressive strength (N/mm^2) … ..	f'_c = 40.72
Tensile strength (N/mm^2) … …	……f_t = 3.7
Tension stiffening	α_1 =10
……	α_2 = 0.6
Prestressing steel	
Young's modulus (N/mm^2) ……	E_s =200000
Effective stress (N/mm^2) ……	f_{se} =945
Ultimate stress (N/mm^2) ……	f_{pu} =1860
Area of prestressing Reinforcement(mm^2)..	99.24

4-2-2 Finite element idealization: Due to symmetry, only one half of the beam has been used in the finite element analysis. The half considered was modeled by using 12-quadratic brick elements. The finite element mesh and the boundary conditions imposed at the ends of the beam are shown in Fig.(10).

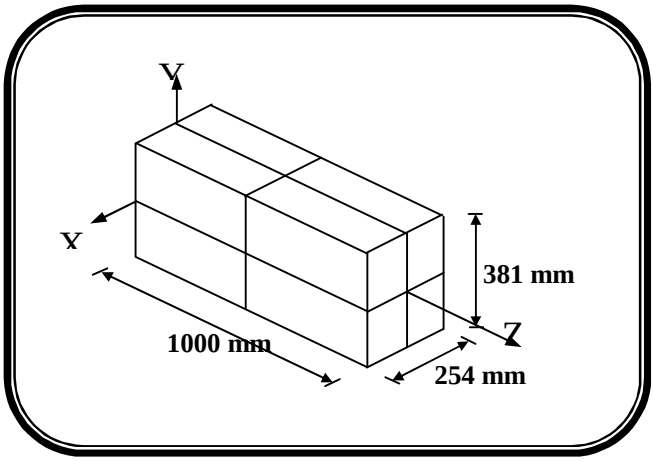

Fig.(10): Wafa et al. (B0.0-2a): finite element mesh (8 elements).

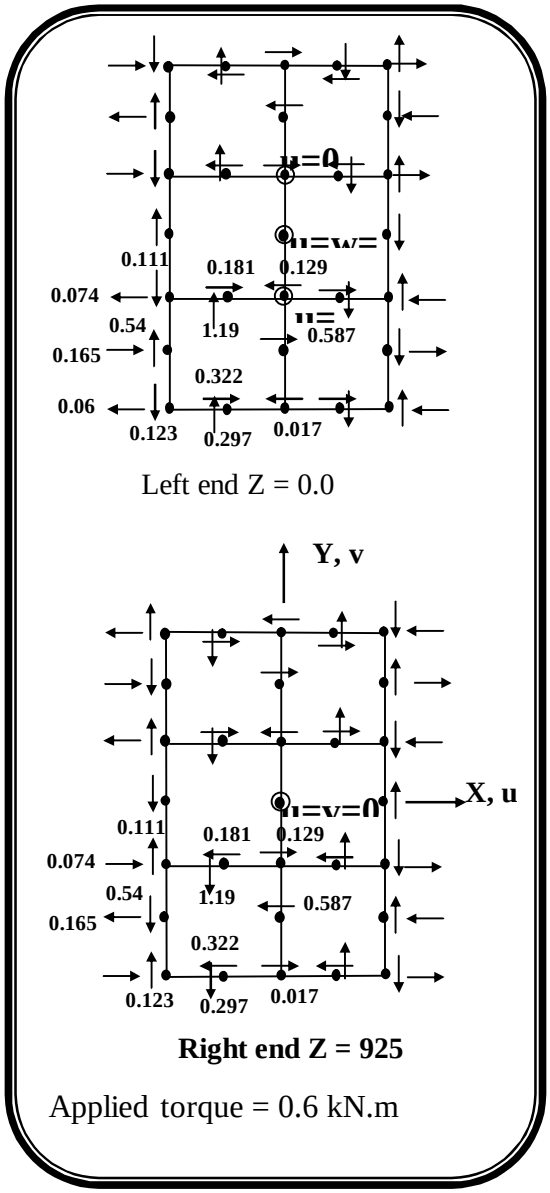

Fig.(11): Wafa et al. (B0.0-2a): Boundary conditions and the equivalent nodal forces.

4-2-3 Results of the analysis: The experimental and numerical torque-twist curves obtained for this beam are shown in Fig.(12). The figure reveal that the finite element solution is in good agreement with experimental results throughout the entire range of behavior. A slightly stiffer numerical response has been observed at post-cracking stage of behavior and the ultimate torque was slightly higher than the experimental value. The numerical ultimate torque was (4.44 kN.m) while the experimental ultimate torque was (4.6 kN.m). The ratio of the predicted ultimate torque to the experimental ultimate torque was (1.036) .

5- Parametric study

The main purpose of the present item was to investigate the effect of several important parameters on the behavior of prestresssed concrete members under torsion.

5-2 Effect of the Degradation of Concrete Compressive Strength

Cervenka's model was adopted in the present work to represent the redaction in the compressive strength of concrete due to the presence of transverse tensile straining after cracking, Cervenka's model includes a compression reduction parameter designated as (k), which is used to control the reduction in the compressive strength, Eq.(3-64). Fig.(13) indicates the analytical torque-angel of twist curves obtained for Hsu beam (P8), using different values for the parameter (k). The figure revels that the effect of the parameter (k) is negligible on the post cracking behavior while it is significantly affect the predicted value of the ultimate torque capacity. The indicates that for k=0, which is the case where the degradation in the compressive strength of concrete is not considered, the predicted torsional capacity is higher than the experimental results. A value of (k) equals to 0.4 gave the best fit to the experimental results.

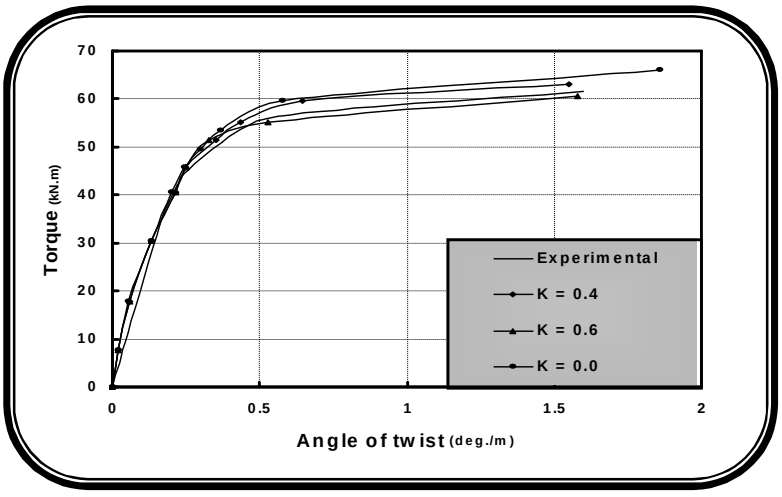

Fig.(13): Hsu beam (P8), effect of the degradation of concrete compressive strength on the torque-angle of twist behavior.

5-2 Influence of the Longitudinal and Transverse Reinforcement:

Fig.(14) exhibits the effect of the variation of amount of longitudinal reinforcement on torque-twist response for Hsu beam (P8). Numerical tests carried out using a total area of longitudinal bars of 516 mm^2, 804 mm^2 and without longitudinal bars. Fig.(15) shows that when the longitudinal steel ratio equals to zero, the predicted ultimate torque is slightly less than the experimental torque, and also it can be noted that when higher longitudinal steel ratio is used the effect of longitudinal steel is negligible on the post cracking behavior and the ultimate torsional capacity was slightly increased.

To study the effect of the amount of transverse reinforcement on the torque-angel of twist behavior and the ultimate torsional capacity, numerical tests carried out using area of stirrups of 31.67, 50.26 and 78.5 mm^2, Fig.(5-10) reveals that the influence of transverse reinforcement substantially affect on the post-cracking torque-angel of twist response.

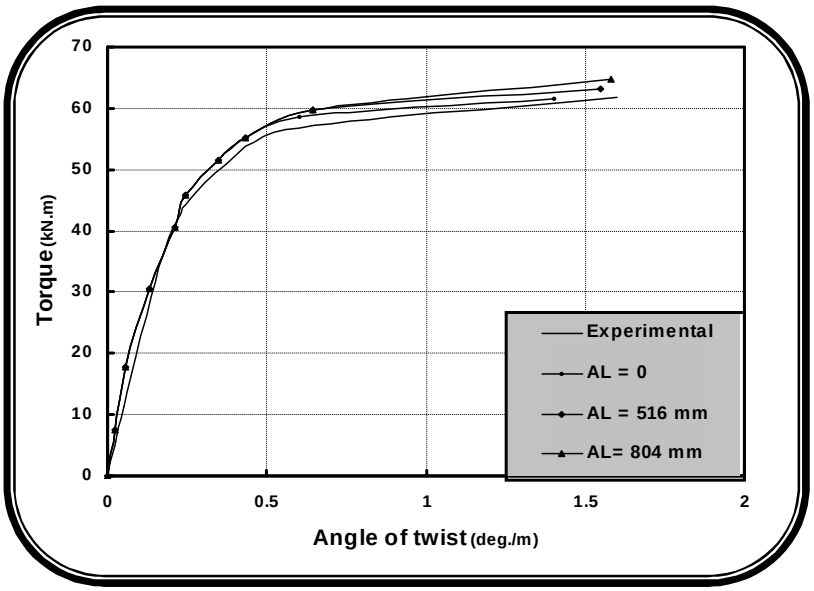

Fig.(14): Hsu beam (P8), ultimate torque for different area of longitudinal steel on the torque-angle of twist behavior.

5-3 Effect of the Prestressing Force:

To study the influence of the prestressing force on the behavior and ultimate torsional capacity of Hsu beam (P8), different values of prestressing force have been considered. The selected values were 0.0, 165.125 kN, 330.25 kN, 495.375 kN, 660.5 kN and 825.625 kN, (for the numerical

analyses 0.0, 0.25, 0.5, 0.75, 1.0, 1.25, times the magnitude of the prestressing force used in experimental work respectively which was f = 660.5 kN). In these analyses the area of prestressing tendon was kept constant. Fig.(16), shows that the magnitude of the prestressing force strongly affects the post-cracking torque-angel of twist curve and ultimate torque. It can be noted that the post cracking response and ultimate torque are substantially increased with higher values of the prestressing force.

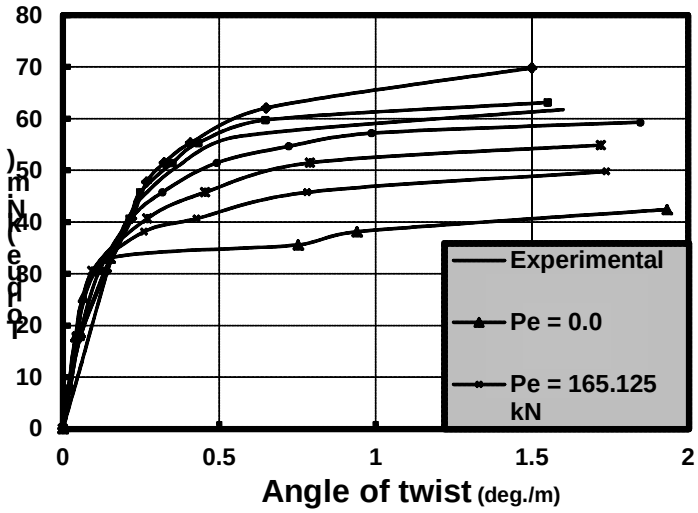

Fig.(16): Hsu beam (P8), effect of prestressing force on the torque-angle of twist behavior.

Effect of Warping Restraint:

In pure torsion analysis, an interesting phenomenon occurs after cracking in which the length of the member increases as the applied torque increases. In this study, beam (P8) is restrained longitudinally at all nodes of end cross sections except the nodes where prestressing force is applied. Fig.(17) shows the torque-angel of twist behavior for pure torsion and torsion with warping restrained. It can be noted that the pre-cracking and post cracking torsional stiffnesses and the collapse torque are considerably increased when the beam is restrained against warping at both ends. The values of the predicted ultimate torque for pure torsion and warping torque are 63.09 kN.m and 91.48 kN.m respectively. The experimental pure torque was 61.7 kN.m therefore. Therefore it can be noted that when the beam is restraint against warping the percentage of increase in the torsional capacity is about 45%.

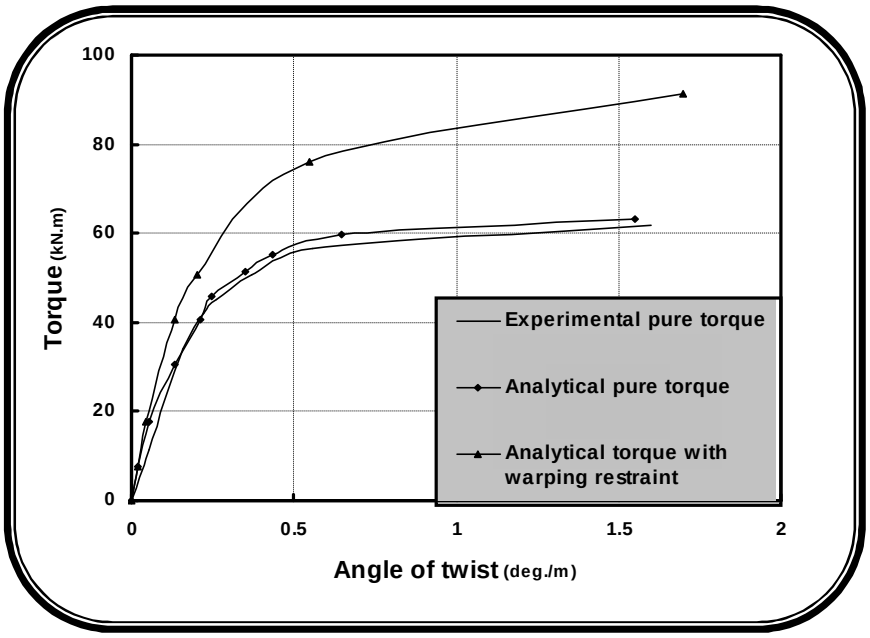

Fig.(17): Hsu beam (P8), effect of the warping restraint on the torque-angle of twist behavior.

5-5 Effect of compressive strength of concrete:

In order to study the effect of increasing the concrete compressive strength on the behavior and ultimate torsional capacity of prestressed concrete beams, Hsu beam (P8) has been analyzed for increased values of the concrete compressive strength. The concrete compressive strengths used in this analysis were, 38.75 MPa ***(1.25*** f_c' **)** and 46.5 MPa **(1.5** f_c' **)** where **(** f_c' **)** is the experimental value **(31 MPa)** of concrete compressive strength. Fig.(18) shows the effect of increasing the compressive strength of concrete on the response of prestressed concrete beams represented by the numerical torque-angel of twist curves. It can be noted that a stiff response in the pre-cracking response and a slight increase in the ultimate torsional capacity is obtained when the value of compressive strength of concrete is increased.

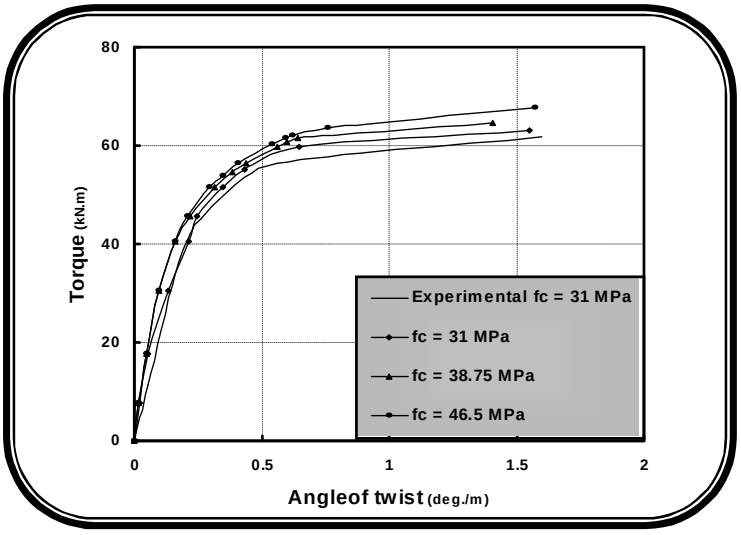

Fig.(18): Hsu beam (P8), effect compressive strength of concrete on the torque-angle of twist behavior.

6 - Conclusions :

1- The Three-dimensional nonlinear finite element model used in the present research work is capable to predict the behavior of prestressed concrete members subjected to torsion. The numerical tests carried out showed that the predicted torque-twist curves are generally in good agreement with the experimental results.

2- It is found that the degradation of the concrete compressive strength due to presence of tensile transverse straining has a negligible effect on the post cracking behavior and significantly affect the predicted value of the ultimate torque. The model used in the present work to account for this phenomenon improves the correlation between the predicted and ultimate capacity of prestressed concrete beams under torsion.

3- At a constant area of prestressing steel, it can be noted that the ultimate torques are substantially increased substantially with the use of higher value of prestressing force. It is found that when the prestressing force is increased by 25%, the ultimate torsional capacity is increased by about 13%.

4- By keeping the amount of transverse steel constant, the increase in the percentage of the longitudinal ordinary reinforcement in presence of prestressing tendon slightly affects the post cracking and slightly increase the value of the ultimate torque.

5- The transverse reinforcement largely effects on the post cracking behavior and the value of the predicted ultimate torque. It can be noted that when the area of transverse reinforcement decrease from 129 mm^2 to 31.67 mm^2, the ultimate torsional capacity is decrease by about 27.58%.

6- The finite element solutions reveal that the prestressed concrete beam casted without web reinforcement have a little ductility, and failure is sudden and violent. The introduce of web reinforcement improves ductility, as well as torsional strength.

7- For prestressed concrete members casted without web reinforcement, the increase in compressive strength of concrete relatively affects the post cracking response and increases the value of the predicted torsional strength. While, for prestressed concrete members provided with web reinforcement, the increase in compressive strength of concrete slightly increases the value of predicted torsional strength.

8- The numerical tests indicate that the post cracking torsional stiffness and the ultimate torque of prestressed concrete beams with warping restraint are considerably higher than those of pure torsion analysis.

7 - Reference:

1- Hsu, T. T. C., ”Torsion of Reinforced Concrete” , Van Nostrand Reinhold Company, New York, 1984.

2- Nilson, A. H., ”Design of Prestressed Concrete”, Wiley and Sons, 1987.

3- Hurst, M. K. ,”Prestressed Concrete Design”, Chapman and Hall, 1988.

4- Rausch, E., ”Berechnung des Eisenbetons gegen Verdrehung. (Torsion) and Abscheren (Analysis of Torsion and Shear in Reinforced Concrete) julius springer. Berlin. Germany. 1929. Pp.53 Cited by. Elfan, L., Karlsson, I., and Losbeg, A., “Torsion-Bending-Shear Interaction for Concrete Beams”, Journal of the Structural Division, ASCE, Vol.100, No.ST8, Proc. Paper 10749, Aug. 1974, pp 1657-1676.

5- Al-Shaarbaf, I. A. S., ”Three-Dimensional Non-Linear Finite Element Analysis of Reinforced Concrete Beams in Torsion”, Ph.D. Thesis University of Bradford, 1990

6- Karlsson, I., "Torsional Stiffening of Reinforced Concrete Structural in Pure Torsion", Report 71:1, Division of Concrete Structural, Chalmers University of Technology, Goterbog, Sweden. June 1971. pp104. Cited by. Elfen, L., Karlsson, I., and Losbeg, A., "Torsion-Bending-Shear Interaction for concrete Beams "Journal of the Structural Division, ASCE, Vol. 100, No.ST8, Proc. Paper 10749, Aug, 1974, pp 1657-1676.

7- Mcmullen. A. E., and Warwaruk, J., "Concrete Beams in Bending, Torsion and Shear", Journal of the Structural Division, ASCE, Vol. 96, No. ST5, Proc. Paper 7270, may, 1970, pp. 885-903. Cited by. Elfen, L., Karlsson, I., and Losbeg, A., "Torsion-Bending-shear interaction for Concrete beams", Journal of the Structural Division, ASCE, Vol. 100, No. St8, Proc. Paper 10749, Aug. 1974, pp. 1657-1676.

8- Chen, W. F., "Plasticity in Reinforced Concrete ", Mcgraw-Hill, 1982, 592 pp.

9- Pognani, T., Slater, J., Anneur-Mosor, R. and Boyukozurk, O., "A Nonlinear Three-Dimensional of Steel Fiber Reinforced Concrete based on Bounding Surface Model", Journal of computer & Structures, Vol. 43, No. 1, 1992, pp. 1-12.

10- Al-bahadly, H. M. A., "Nonlinear Analysis of Elasto-Plastic Steel and Reinforced Concrete beams in Torsion using Three-Dimensional Finite Element model", M. Sc. Thesis, University of Technology, Baghdad, 1995.

11- Al-Zahowi, S. K., "Nonlinear Finite Element Analysis of Reinforced Concrete Voided Slab Strips", M. Sc. Thesis, University of Technology, Baghdad, 1999.

12- Allose, L. E. H., "Three-Dimensional Nonlinear Finite Element Analysis of Steel Fiber Reinforced Concrete beams in Torsion", M. Sc. Thesis, University of Technology, Baghdad, 1995.

13- Hsu, T. T. C., "Softening of Concrete in Torsional members-Prestressed Concrete," Journal of American Concrete Institute, September-October 1985, pp. 603-615.

14- Wafa, F. F., Abul Hasnat, and Tarabolsi, O. F., "Prestressed Fiber Reinforced Concrete beams Subjected to Torsion," ACI Structural Journal, May-June 1992, pp. 272-283.

15- Belarbi, A., and Hsu, T. T. C., "Constitutive Laws of Softened Concrete in Biaxial Tension-Compression", ACI Structural Journal, Sept.-Oct. 1995, pp. 562-573.

16- Hsu, T. T. C., "Softened Truss Model Theory Shear and Torsion", ACI Structural Journal, Vol. 85, dec. 1988, pp. 624-635.

17- Hsu, T. T. C., "Softened Truss Model Theory Shear and Torsion", ACI Structural Journal, Vol. 85, dec. 1988, pp. 624-635.

18- Vecchio, F. J., Collins M. P. and Aspiotis, J., "High Strength Concrete Element Subjected to shear", ACI Structural Journal, July-Aug. 1994, pp. 423-433.

19- Hsu, T. T. C., Mo, Y. L., "Softened of Concrete in Torsional members-Theory and Test", ACI Journal, Vol. 82, no. 3, May-June 1985, pp. 290-203

20- Robinson, J. R. and Demorieux, J. M., "Essaais De Traction-Compression Sur Models Dame De Poutre en Beton Arme", Institute de Recherches Appliquees Dui Beton Arme (IRABA), Part 1, June 1968 and Part 2, May 1972. Cited by Al-Shaarbaf, I. A. S. ,"Three-Dimensional Non-Linear Finite Element Analysis of Reinforced Concrete Beams in Torsion", Ph.D. Thesis University of Bradford, 1990

21- Vecchio, F., and Collins, M. P., "The Response of Reinforced Concrete Equation Torsion In-plane Shear and Normal Stresses", Publication No. 82-103, University of Toronto, Canada, 1982.